"CLL pathogenesis: a cooperation between microenvironments and genetics"

Carlo M. Croce, M.D.

The Ohio State University
Distinguished University Professor
The John W. Wolfe Chair in Human Cancer Genetics
Director, Institute of Genetics
Director, Human Cancer Genetics Program

1st POSTGRADUATE
CLL Conference
Bologna,
November
13-14 2017

Royal Hotel Carlton

Presidents: Robin Foà , Pier Luigi Zinzani

Disclosures of Carlo M. Croce, M.D.

Company name	Research support	Employee	Consultant	Stockholder	Speakers bureau	Advisory board	Other
N/A							

Occurrence of the most frequent and recurrent chromosomal abnormalities in human CLL

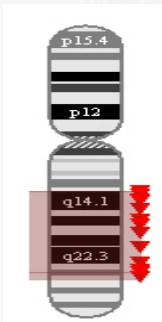

11q23

18 %

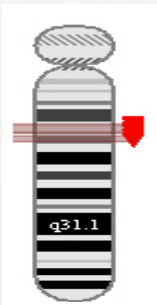

13q14

55 %

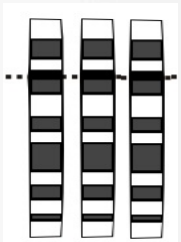

Trisomy 12

12 %

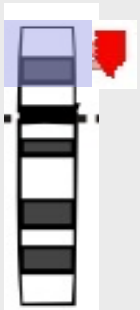

17p13

7%

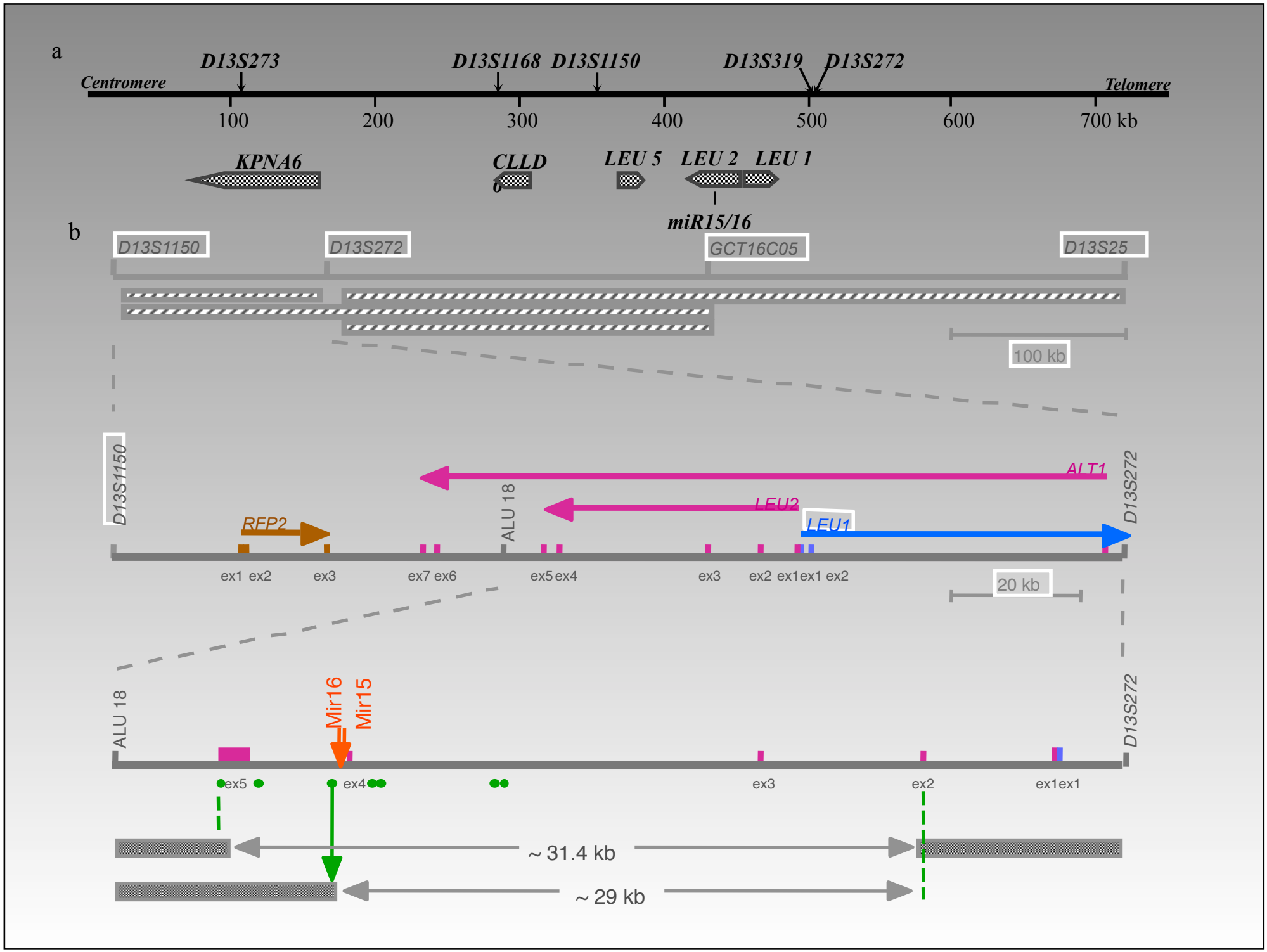
a
D13S273
D13S1168
D13S1150
D13S319
D13S272
Centromere
Telomere
100
200
300
400
500
600
700 kb
KPNA6
CLLD 6
LEU 5
LEU 2
LEU 1
miR15/16
b
D13S1150
D13S272
GCT16C05
D13S25
100 kb
D13S1150
ALT1
LEU2
LEU1
RFP2
ALU 18
D13S272
ex1 ex2
ex3
ex7 ex6
ex5 ex4
ex3
ex2 ex1ex1 ex2
20 kb
ALU 18
Mir16
Mir15
D13S272
ex5
ex4
ex3
ex2
ex1ex1
~ 31.4 kb
~ 29 kb

Genetic variations in the genomic sequences of miRNAs in CLL patients *.

miRNA	Location **	CLL	Normals	miRNACHIP expression	Observation
miR-16-1	Germline pri-miRNA (CtoT)+7bp in 3'	2/75	0/160	Reduced to 15% and 40% of normal, respectively	Normal allele deleted in CLL cells in both patients (FISH, LOH); For one patient: Previous breast cancer; Mother died with CLL; sister died with breast ca;
miR-27b	Germline pri-miRNA (GtoA)+50bp in 3'	1/75	0/160	Normal	Mother throat and lung cancer at 58. Father lung cancer at 57.
miR-29b-2	pri-miRNA (GtoT)+212 in 3'	1/75	0/160	Reduced to 75%	Sister breast cancer at 88 (still living). Brother "some type of blood cancer" at 70.
miR-29b-2	pri-miRNAs ins (+A)+107 in 3'	3/75	0/160	Reduced to 80%	For two patients: Fam history of unspecified cancer
miR-187	pri-miRNA (TtoC)+73 in	1/75	0/160	NA	Unknown
miR-206	pre-miRNA 49(GtoT)	2/75	0/160	Reduced to 25%	Prostate cancer; mother esophogeal cancer. Brother prostate cancer sister breast cancer
miR-206	Somatic pri-miRNA (AtoT)-116 in 5'	1/75	0/160	Reduced to 25% (data only for one pt)	Aunt some type of leukemia (dead)
miR-29c	pri-miRNA (GtoA)31 in 5'	2/75	1/160	NA	Paternal grandmother CLL; sister breast ca. (one pt).
miR-122a	pre-miRNA 53(CtoT)	1/75	2/160	Reduced to 33%	Paternal uncle colon cancer.
miR-187	pre-miRNA 34(GtoA)	1/75	1/160	NA	Grandfather polycythemia vera. Father a history of cancer but not lymphoma.

Note: * - For each patient/normal control more than 12kb of genomic DNAs was sequenced and, in total, we screened by direct sequencing ~627kb of tumor DNA and about 700kb of normal DNA. The position of the mutations are reported in respect with the precursor miRNA molecule. The list of 42 microRNAs analyzed includes 15 members of the specific signature or members of the same clusters, *miR-15a, miR-16-1, miR-23a, miR-23b, miR-24-1, miR-24-2, miR-27a, miR-27b, miR-29b-2, miR-29c, miR-146, miR-155, miR-221, miR-222, miR-223* and 27 other microRNAs (randomly selected): *let-7a2, let-7b, miR-17-3p, miR-17-5p, miR-18, miR-19a, miR-19b-1, miR-20, miR-21, miR-30b, miR-30c-1, miR-30d, miR-30e, miR-32, miR-100, miR-105-1, miR-108, miR-122, miR-125b-1, miR-142-5p, miR-142-3p, miR-193, miR-181a, miR-187, miR-206, miR-224, miR-346.*

** - When normal correspondent DNA from bucal mucosa was available, the alteration was identified as germline when present or somatic when absent, respectively. FISH = fluorescence *in situ* hybridization; LOH = loss of heterozygosity; NA = not available

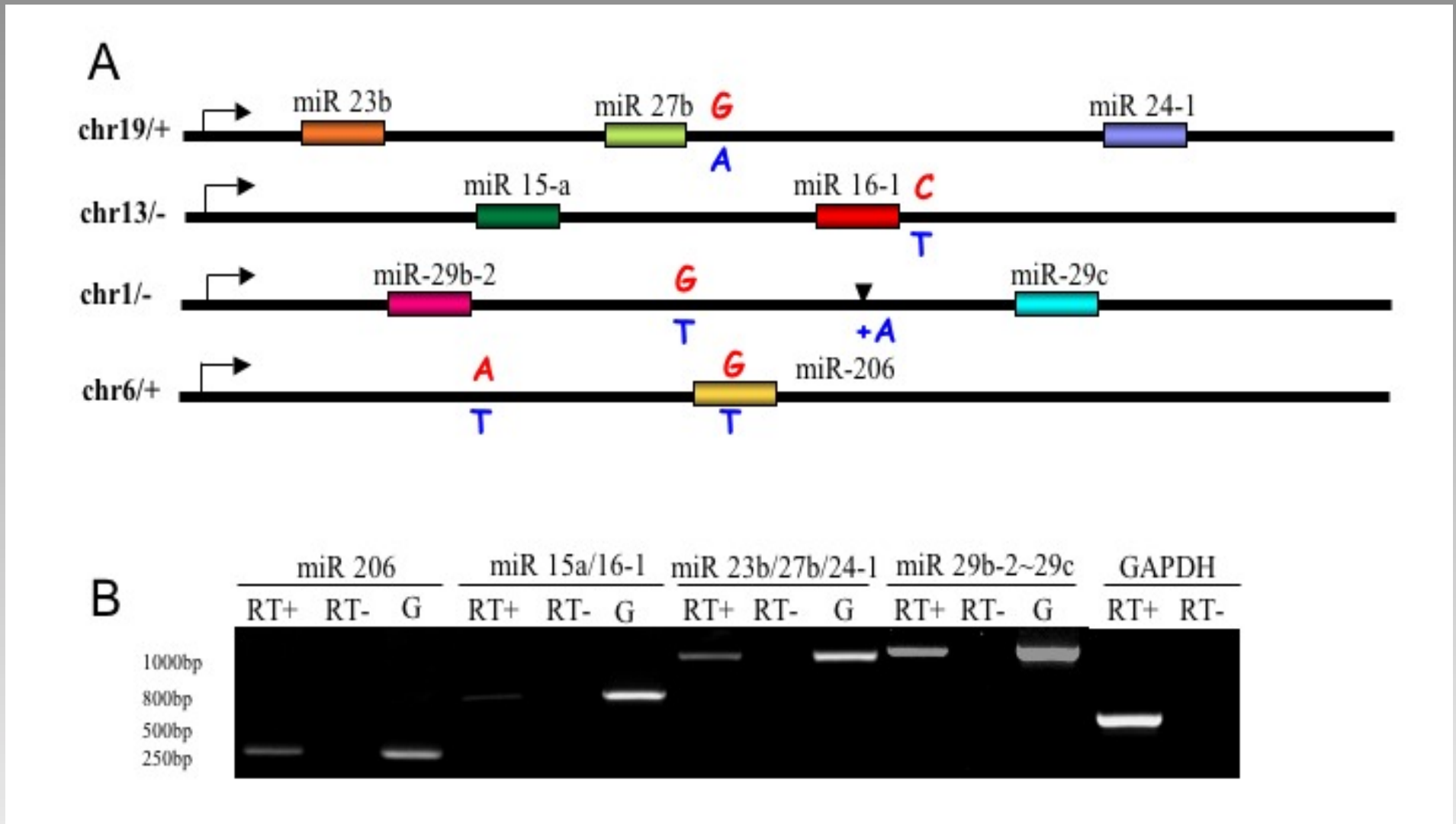
A
chr19/+
miR 23b
miR 27b
G
A
miR 24-1
chr13/-
miR 15-a
miR 16-1
C
T
chr1/-
miR-29b-2
G
T
+A
miR-29c
chr6/+
A
T
G
T
miR-206
B
miR 206
miR 15a/16-1
miR 23b/27b/24-1
miR 29b-2~29c
GAPDH
RT+ RT- G RT+ RT- G RT+ RT- G RT+ RT- G RT+ RT-
1000bp
800bp
500bp
250bp

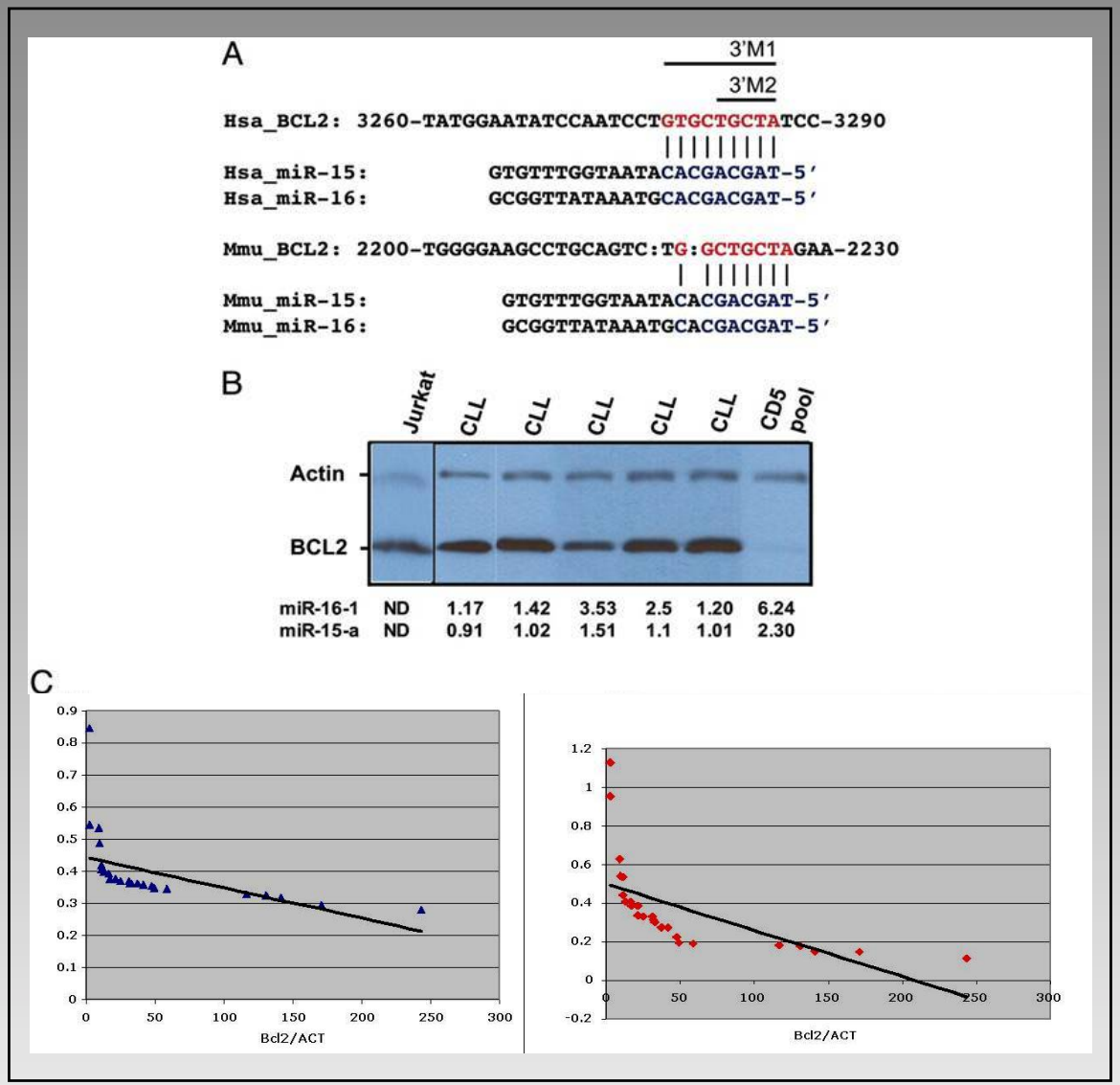

Bcl2 protein expression is inversely correlated with *miR-15a* and *miR-16-1* miRNAs expression in CLL patients. (*A*) The unique site of complementarity miR::mRNA is conserved in human and mouse and is the same for all four human m protein are inversely correlated with *miR-15a* and *miR-16-1* expression. Five different CLL cases are presented, and the normal cells were pools of $CD5^+$ B lymphocytes. The T cell leukemia Jurkat was used as control for Bcl2 protein expression. For normalization we used β-actin. The numbers represent normalized expression on miRNACHIP. ND, not determined. (*C*) The inverse correlation in the full set of 26 samples of CLL between miR-15a / miR-16-1 and Bcl2 protein expressions. The normalized Bcl2 expression is on abscissa vs. *miR-15a* (*Left*) and *miR-16-1* (*Right*) levels by miRNA chip on ordinates. ACT, β-actin.

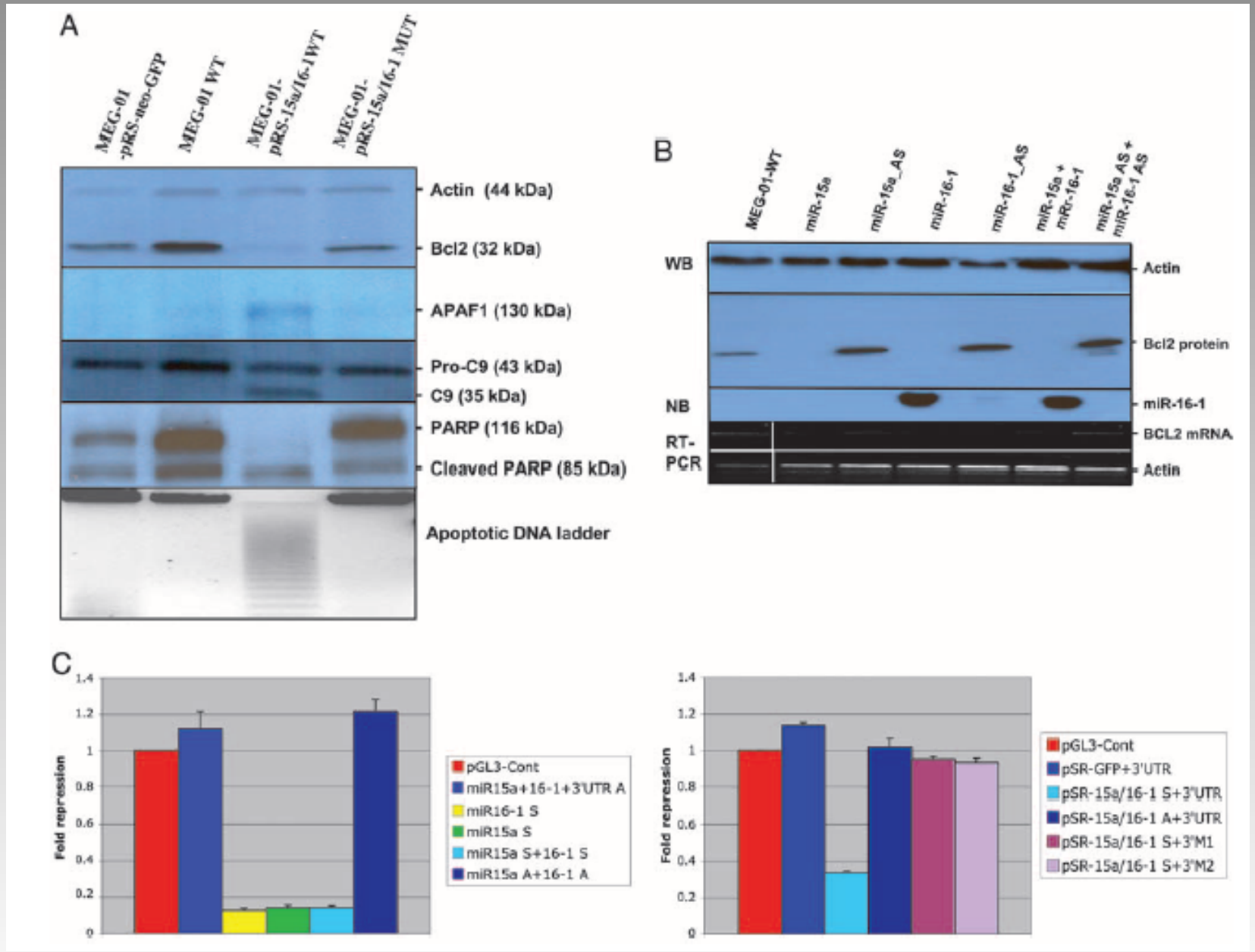
A
MEG-01 pRS-neo-GFP
MEG-01 WT
MEG-01-pRS-15a/16-1WT
MEG-01-pRS-15a/16-1 MUT
Actin (44 kDa)
Bcl2 (32 kDa)
APAF1 (130 kDa)
Pro-C9 (43 kDa)
C9 (35 kDa)
PARP (116 kDa)
Cleaved PARP (85 kDa)
Apoptotic DNA ladder
B
MEG-01-WT
miR-15a
miR-15a_AS
miR-16-1
miR-16-1_AS
miR-15a + miR-16-1
miR-15a AS + miR-16-1 AS
WB
NB
RT-PCR
Actin
Bcl2 protein
miR-16-1
BCL2 mRNA
Actin
C
Fold repression
1.4
1.2
1
0.8
0.6
0.4
0.2
0
pGL3-Cont
miR15a+16-1+3'UTR A
miR16-1 S
miR15a S
miR15a S+16-1 S
miR15a A+16-1 A
Fold repression
1.4
1.2
1
0.8
0.6
0.4
0.2
0
pGL3-Cont
pSR-GFP+3'UTR
pSR-15a/16-1 S+3'UTR
pSR-15a/16-1 A+3'UTR
pSR-15a/16-1 S+3'M1
pSR-15a/16-1 S+3'M2

nature medicine

ABT-199, a potent and selective BCL-2 inhibitor, achieves antitumor activity while sparing platelets

Andrew J Souers[1], Joel D Leverson[1], Erwin R Boghaert[1], Scott L Ackler[1], Nathaniel D Catron[1], Jun Chen[1], Brian D Dayton[1], Hong Ding[1], Sari H Enschede[1], Wayne J Fairbrother[2], David C S Huang[3,4], Sarah G Hymowitz[2], Sha Jin[1], Seong Lin Khaw[3,4], Peter J Kovar[1], Lloyd T Lam[1], Jackie Lee[2], Heather L Maecker[2], Kennan C Marsh[1], Kylie D Mason[3–5], Michael J Mitten[1], Paul M Nimmer[1], Anatol Oleksijew[1], Chang H Park[1], Cheol-Min Park[1,7], Darren C Phillips[1], Andrew W Roberts[3–5], Deepak Sampath[2], John F Seymour[4,6], Morey L Smith[1], Gerard M Sullivan[1], Stephen K Tahir[1], Chris Tse[1], Michael D Wendt[1], Yu Xiao[1], John C Xue[1], Haichao Zhang[1], Rod A Humerickhouse[1], Saul H Rosenberg[1] & Steven W Elmore[1]

Proteins in the B cell CLL/lymphoma 2 (BCL-2) family are key regulators of the apoptotic process. This family comprises proapoptotic and prosurvival proteins, and shifting the balance toward the latter is an established mechanism whereby cancer cells evade apoptosis. The therapeutic potential of directly inhibiting prosurvival proteins was unveiled with the development of navitoclax, a selective inhibitor of both BCL-2 and BCL-2–like 1 (BCL-X_L), which has shown clinical efficacy in some BCL-2–dependent hematological cancers. However, concomitant on-target thrombocytopenia caused by BCL-X_L inhibition limits the efficacy achievable with this agent. Here we report the re-engineering of navitoclax to create a highly potent, orally bioavailable and BCL-2–selective inhibitor, ABT-199. This compound inhibits the growth of BCL-2–dependent tumors *in vivo* and spares human platelets. A single dose of ABT-199 in three patients with refractory chronic lymphocytic leukemia resulted in tumor lysis within 24 h. These data indicate that selective pharmacological inhibition of BCL-2 shows promise for the treatment of BCL-2–dependent hematological cancers.

Apoptosis, or programmed cell death, is a conserved and regulated process that is the primary mechanism for the removal of aged, damaged and unnecessary cells. The ability to block apoptotic signaling is a key hallmark of cancer and is thus important for oncogenesis, tumor maintenance and chemoresistance[1]. Dynamic binding interactions between prodeath (for example, BCL-2–associated X protein (BAX), BCL-2 antagonist/killer 1 (BAK), BCL-2–associated agonist of cell death (BAD), BCL-2–like 11 (BIM), NOXA and BCL-2 binding component 3 (PUMA)) and prosurvival (BCL-2, BCL-X_L, BCL-2–like 2 (BCL-W), myeloid cell leukemia sequence 1 (MCL-1) and BCL-2–related protein A1 (BFL-1)) proteins in the BCL-2 family control commitment to programmed cell death. Altering the balance among these opposing factions provides one means by which cancer cells undermine normal apoptosis and gain a survival advantage[2,3].

BCL-2, the first identified apoptotic regulator, was originally cloned from the breakpoint of a t(14;18) translocation present in human B cell lymphomas[2,4–6]. This protein has since been shown to have a dominant role in the survival of multiple lymphoid malignancies[7,8]. BCL-X_L was subsequently identified as a related prosurvival protein and is associated with drug resistance and disease progression of multiple solid-tumor and hematological malignancies[5,9,10]. We have previously established that BCL-X_L is also the primary survival factor in platelets[11,12]. Genetic ablation, hypomorphic mutation or pharmacologic inhibition of BCL-X_L results in reduced platelet half-life and dose-dependent thrombocytopenia *in vivo*[12].

The association of prosurvival BCL-2 family members with tumor initiation, disease progression and drug resistance makes them compelling targets for antitumor therapy[2]. Despite the fact that direct antagonism of proteins in the BCL-2 family requires disruption of protein-protein interactions, the use of structure-based drug design has recently rendered these proteins tractable targets[13]. We previously reported navitoclax (ABT-263), an orally bioavailable small molecule with a high affinity for both BCL-2 and BCL-X_L that is currently being evaluated in phase 2 clinical trials[14–18]. Both the antitumor efficacy and hematologic toxicities of navitoclax are dictated by its inhibition profile of prosurvival proteins in the BCL-2 family. Early signs of clinical antitumor activity have been observed in lymphoid malignancies thought to be dependent on BCL-2 for survival[16,17]. As predicted by preclinical data, inhibition of BCL-X_L by navitoclax induces a rapid, concentration-dependent decrease in the number

[1]AbbVie Inc., North Chicago, Illinois, USA. [2]Genentech, Inc., South San Francisco, California, USA. [3]The Walter and Eliza Hall Institute of Medical Research, Parkville, Victoria, Australia. [4]Faculty of Medicine, Dentistry and Health Sciences, University of Melbourne, Melbourne, Victoria, Australia. [5]Department of Clinical Hematology and Bone Marrow Transplantation, Royal Melbourne Hospital, Parkville, Victoria, Australia. [6]Department of Hematology, Peter MacCallum Cancer Centre, Melbourne, Victoria, Australia. [7]Present address: Division of Chemistry and Biological Chemistry, School of Physical and Mathematical Sciences, Nanyang Technological University, Singapore. Correspondence should be addressed to A.J.S. (andrew.souers@abbvie.com).

Received 17 July 2012; accepted 29 November 2012; published online 6 January 2013; doi:10.1038/nm.3048

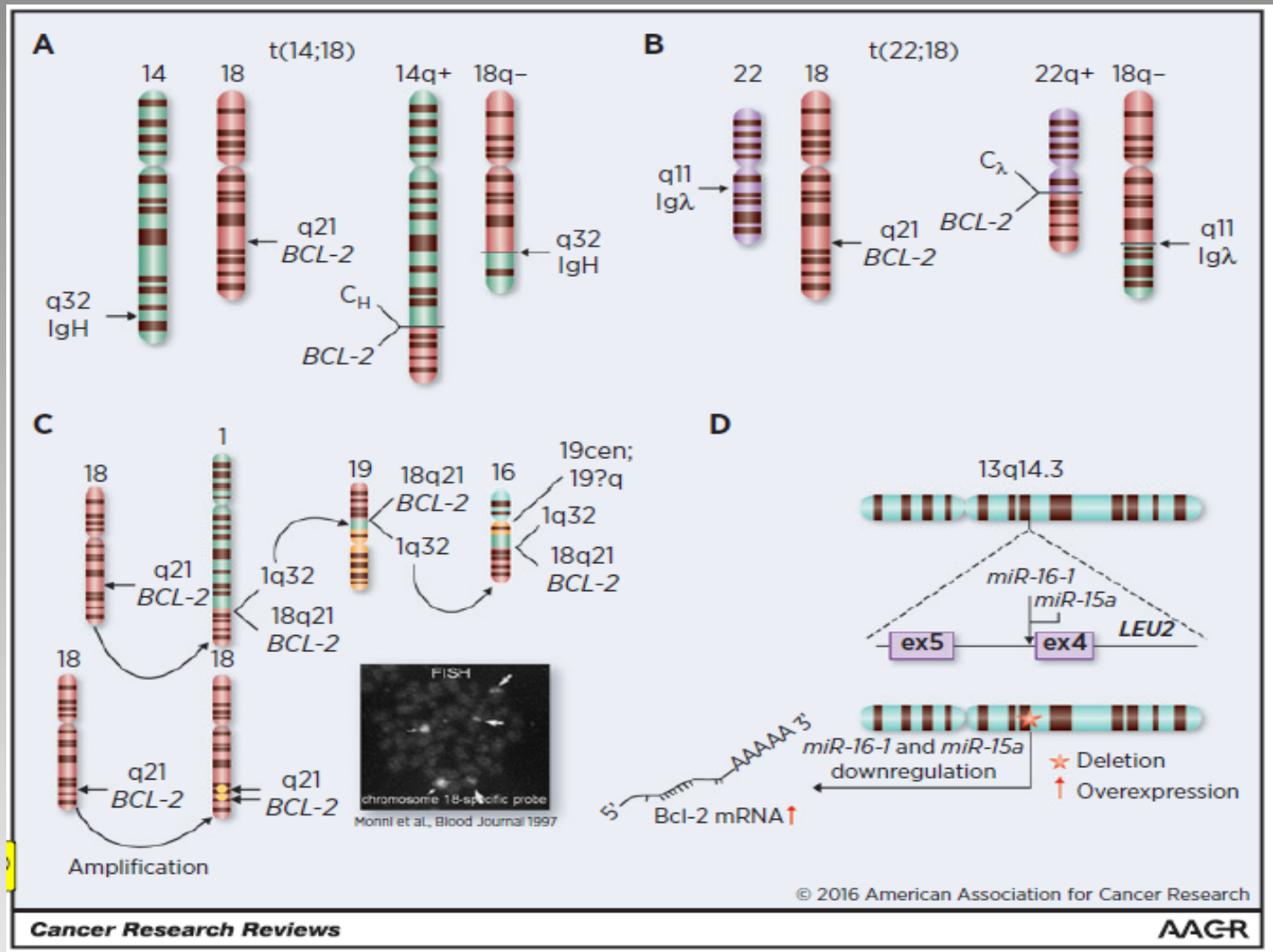

Figure 1.
Genetic lesions accounting for dysregulation of *BCL-2* gene expression in malignancies. **A,** the t(14;18) and the t(22;18) reciprocal chromosome translocations (**B**) are depicted. The translocations juxtapose the *BCL-2* gene to enhancer elements of the Ig loci causing deregulation of expression of *BCL-2*. **C,** *BCL-2* gene amplification schemes. Top, chromosome 18q–derived sequences are depicted with translocation to chromosome 1q32, which was further translocated to chromosomes 19 and 16. FISH using a chromosome 18-specific probe shows *BCL-2* amplification, three labels (large arrows) in addition to normal chromosomes (small arrows). Bottom, *BCL-2* gene amplification without chromosome rearrangements (**D**) The 13q14 genomic region is deleted in most CLLs. The genes encoding miR-15a and miR-16-1 lie within a 30-kb deleted region between exons 2 and 5 of the *DLEU2* gene. The deletion of miR-15a and miR-16-1 locus leads to Bcl-2 mRNA overexpression.

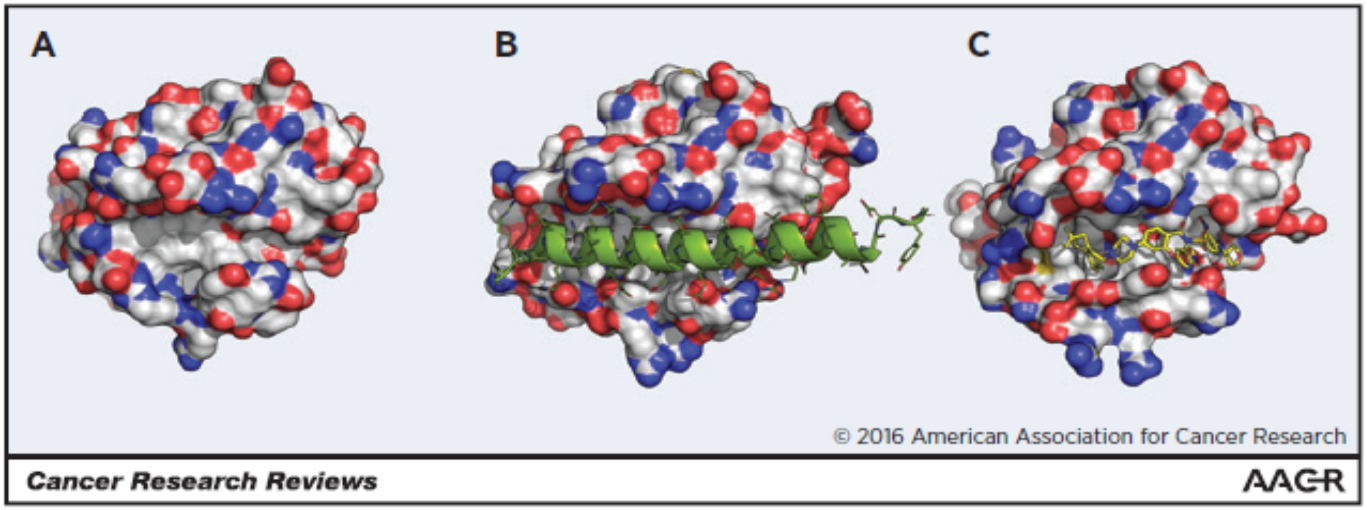

Figure 2.

Three-dimensional structure of antiapoptotic Bcl-2 family members. The 3D structure of the human Bcl-XL protein is depicted with an empty groove (**A**; PDB accession code: 1MAZ) and in complex with the BH3 peptide from Bim (**B**; PDB accession code: 1PQ1). The human Bcl-2 protein is represented in complex with a modeled structure of venetoclax based on the crystal structure of (4-(4-{[4-(4-chlorophenyl)-5,6-dihydro-2H-pyran-3-yl]methyl}piperazin-1-yl)-N-{[3-nitro-4-(tetrahydro-2H-pyran-4-ylamino)phenyl]sulfonyl}benzamide), a close analog (**C**; PDB accession code: 4MAN). The Connolly surface of the proteins is colored by mapped atom type (carbon, white; nitrogen, blue; oxygen, red; sulfur, yellow).

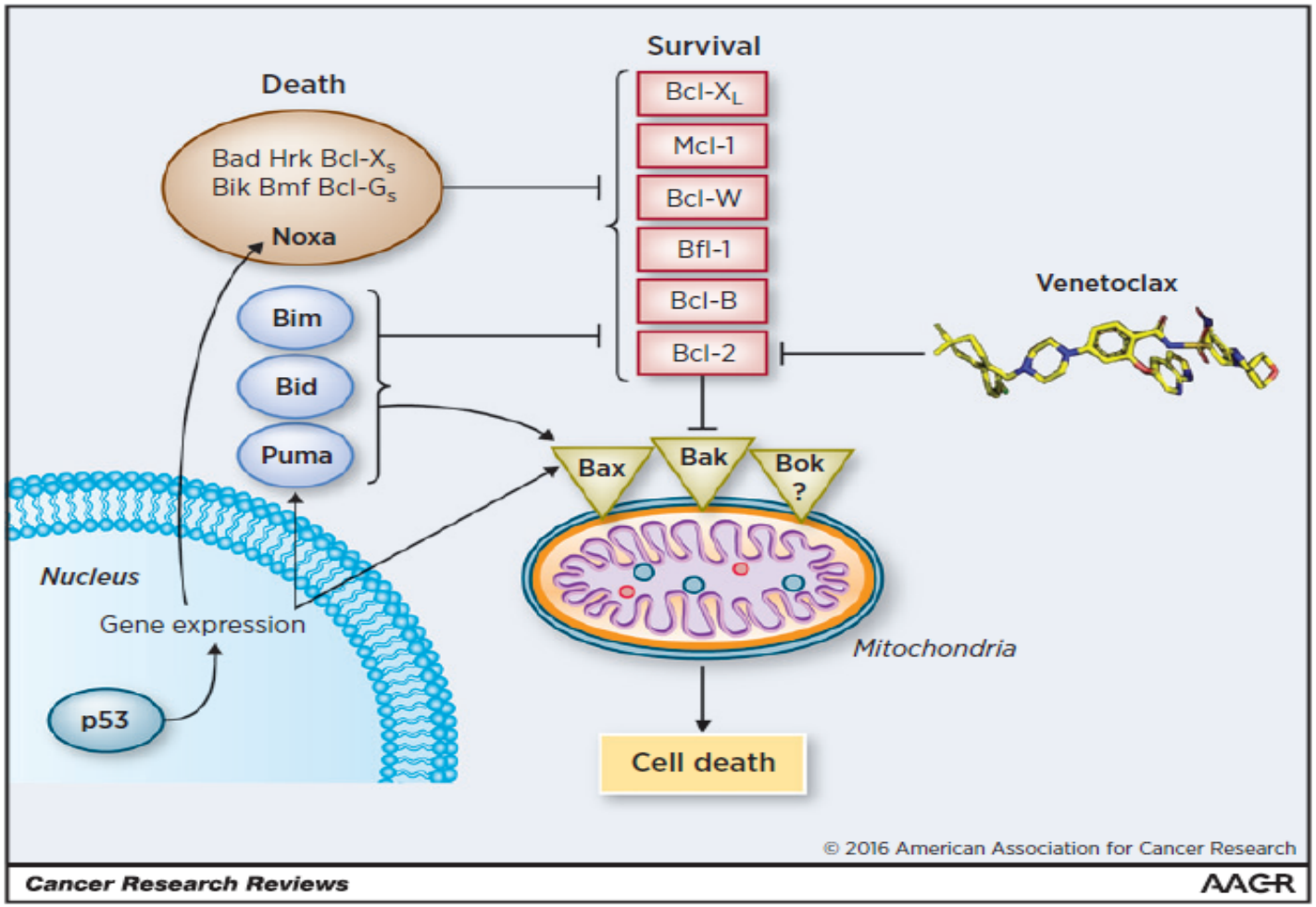

Figure 3.
Interactions among Bcl-2 family proteins. The categories of the Bcl-2 family are represented, including: (i) anti-apoptotic proteins, Bcl-2, Bcl-XL, Mcl-1, Bcl-W, Bfl-1, and Bcl-B (red); (ii) the multi-domain proapoptotic, Bax, Bak, and possibly Bok (yellow), which permeabilize the outer mitochondrial membrane; (iii) BH3-only proteins that operate as both agonists of proapoptotic Bax/Bak and antagonists of anti-apoptotic Bcl-2 members (pink); and (iv) BH3-containing proapoptotic members that operate as antagonists of the antiapoptotic proteins (orange). Tumor suppressor p53 plays important roles in responses to chemotherapy and stimulates transcription of specific proapoptotic members of the family (*BAX, PUMA, BID, NOXA*). Venetoclax is a selective antagonist of Bcl-2.

1984	14 ; 18 breakpoint cloned
1985-1986	Bcl-2 cDNA cloned ; sequenced
1988	Apoptosis suppression
1989	Bcl-2 poor progress in NHL
1990	Bcl-2 localized to mitochondria
1992	Chemoresistance
1993	Bax dimerizes with Bcl-2
1993	Bcl-2 over expressed in CLL
1993	ASO reverses chemoresistance
1994	Mitochondria required
1996	BH3 mediates dimerization
1996	Bcl-X 3D structure
1997	Bcl-2 ASO (Ph3 CLL)
1997	Bcl-XL + BH3 3D structure
1997	Bcl-2 gene amplified (DLBCL)
1999	SAR by NMR
2001	Bcl-2 3D structure
2002, 2005	MiR15-16 deletion (CLL)
2005	ABT 737 development
2007	Bcl-XL required for platelets
2007	Obatoclax discovered
2008	Navitoclax discovered
2009	Obatoclax Ph 1
2011	Navitoclax Ph 1
2013	Venetoclax discovered
2016	Venetoclax impressive activity in R/R CLL
2016	FDA approval

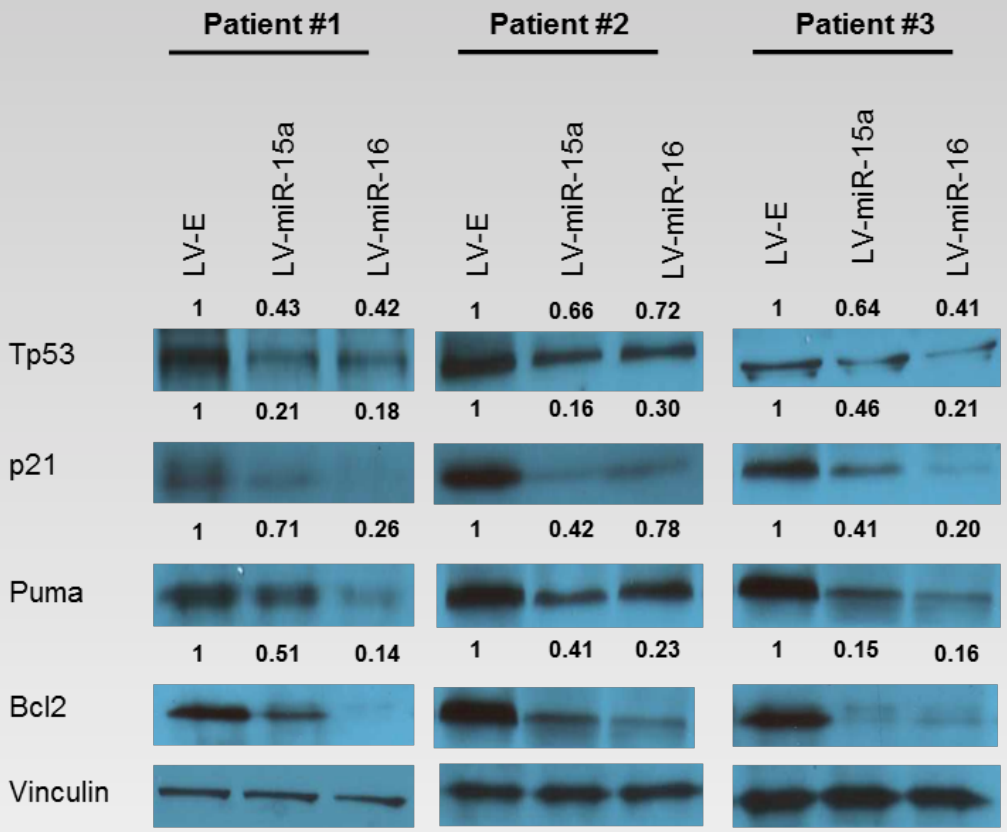

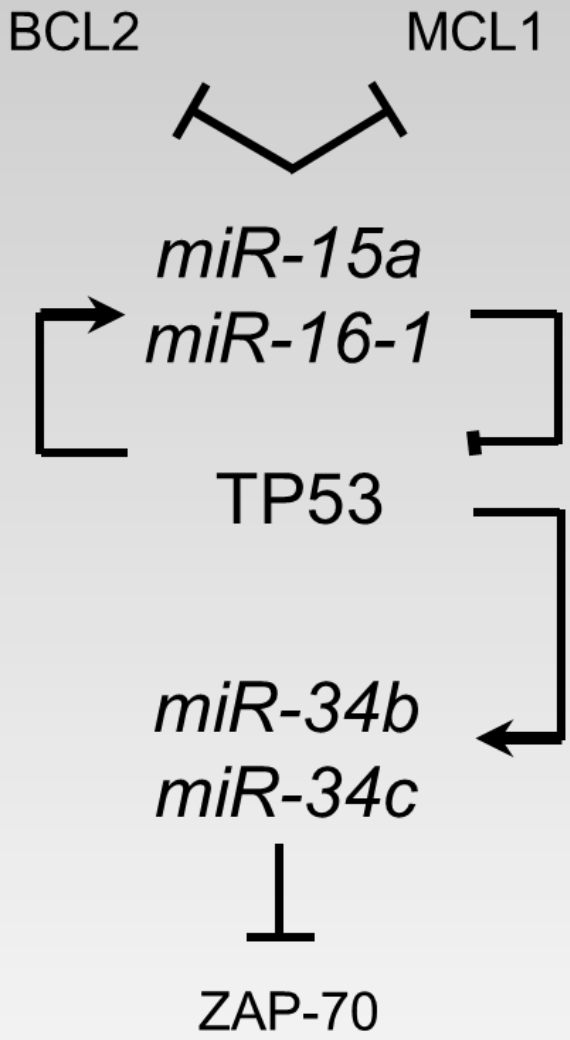

(Fabbri and Botoni et al, JAMA,)

Gene Name	ROR1 low	ROR1 high	LINEAR FC	P value
hsa-miR-199a-5p	62.5	22.1	2.8	0.012
hsa-miR-451a	1653.0	610.4	2.7	0.006
hsa-miR-151a-3p	71.6	29.6	2.4	0.001
hsa-miR-151a-5p	131.6	55.1	2.4	0.001
hsa-miR-484	33.8	14.6	2.3	0.024
hsa-miR-132-3p	34.0	16.0	2.1	0.030
hsa-miR-199a-3p+hsa-miR-199b-3p	231.8	116.6	2.0	0.044
hsa-miR-15a-5p	2600.6	1327.4	2.0	0.006
hsa-miR-365a-3p+hsa-miR-365b-3p	105.9	59.7	1.8	0.043
hsa-miR-363-3p	183.1	107.1	1.7	0.005
hsa-miR-16-5p	18347.2	10848.8	1.7	0.003
hsa-miR-222-3p	1308.6	841.8	1.6	0.004
hsa-miR-337-3p	36.0	56.2	-1.6	0.028
hsa-miR-29a-3p	2011.4	3258.2	-1.6	0.002
hsa-miR-664a-3p	213.0	405.2	-1.9	<0.001
hsa-miR-148a-3p	411.8	1051.9	-2.6	0.009
hsa-miR-155-5p	1829.5	5064.8	-2.8	0.001

Tab. 1. Nanostring results

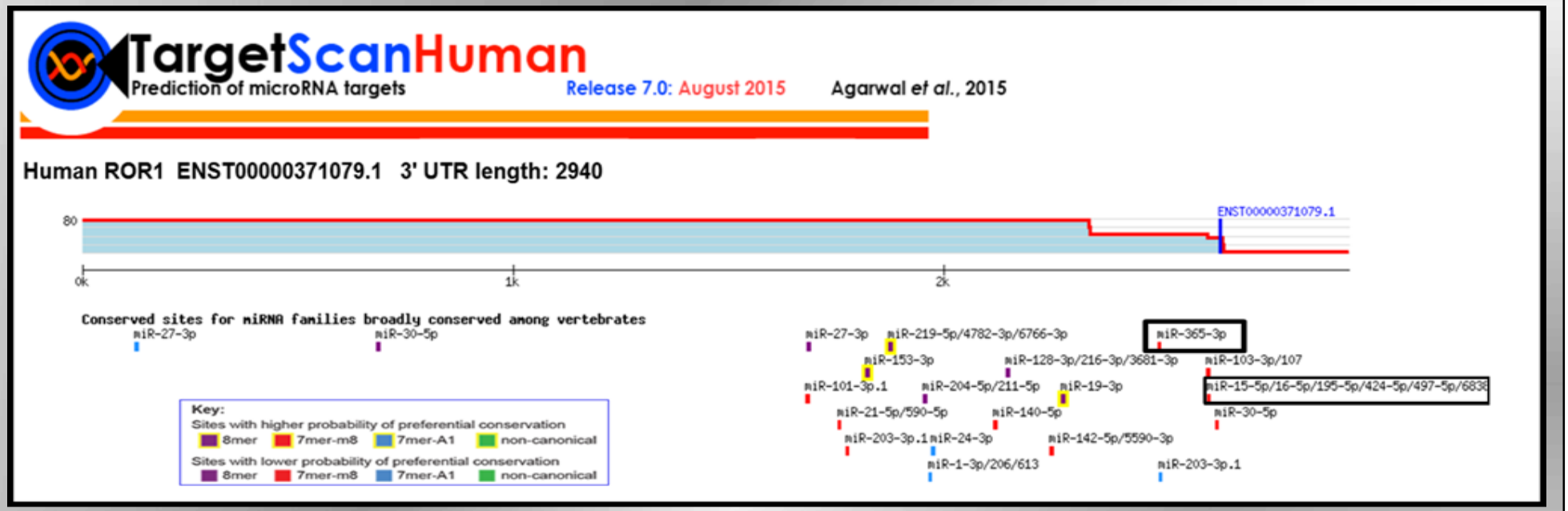

Fig. 2. *Mir-15/16* and *miR-365-3p* are predicted to target the 3'UTR of *ROR1* by targetscan software.

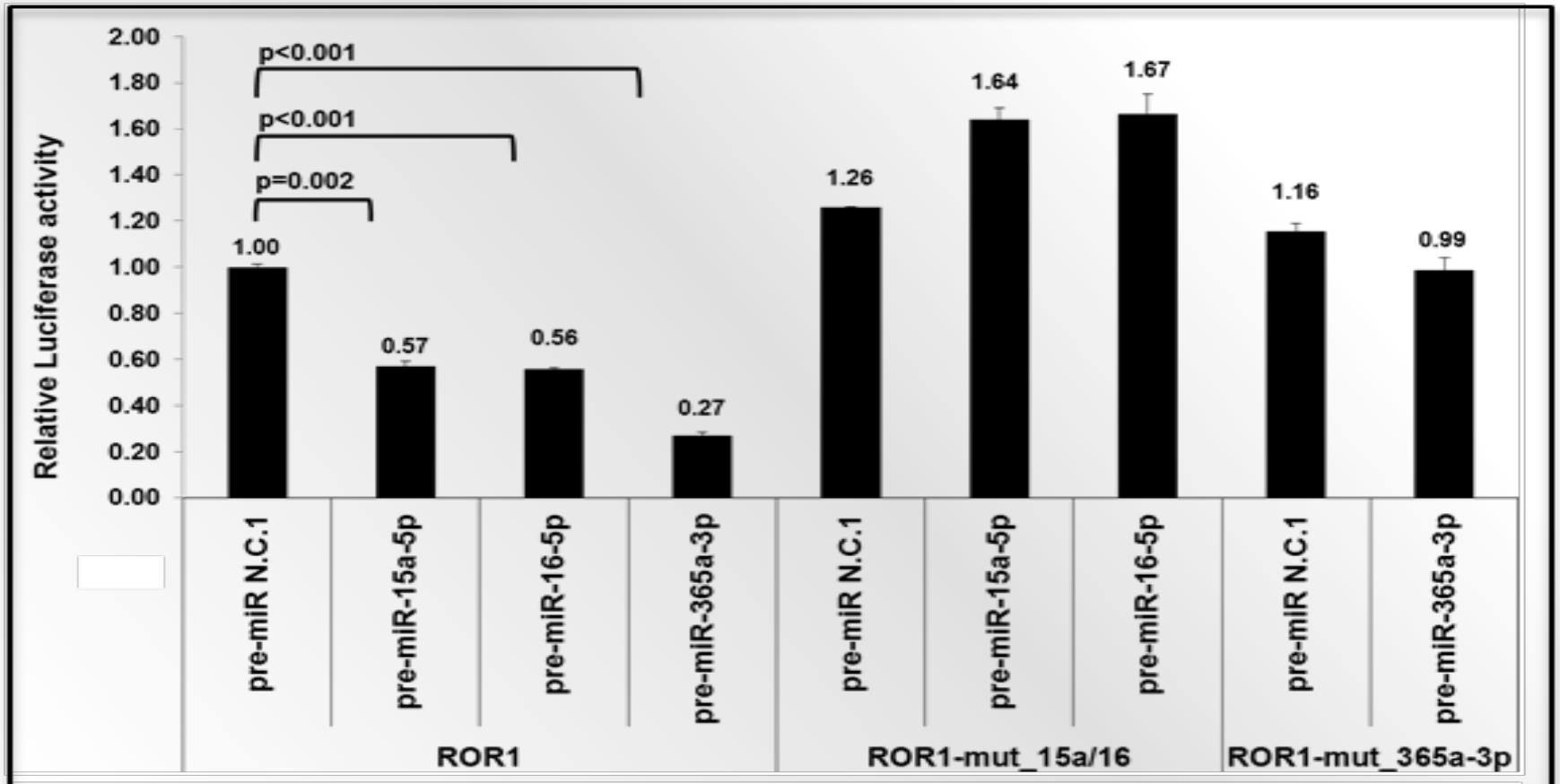

Fig. 3. MiR15/16 targets ROR1 expression.
Transfection experiments were performed in HEK-293 cells using constructs indicated. First four lines show results using WT construct. Lines from 5 to 9 show results using constructs with mutant target sites.

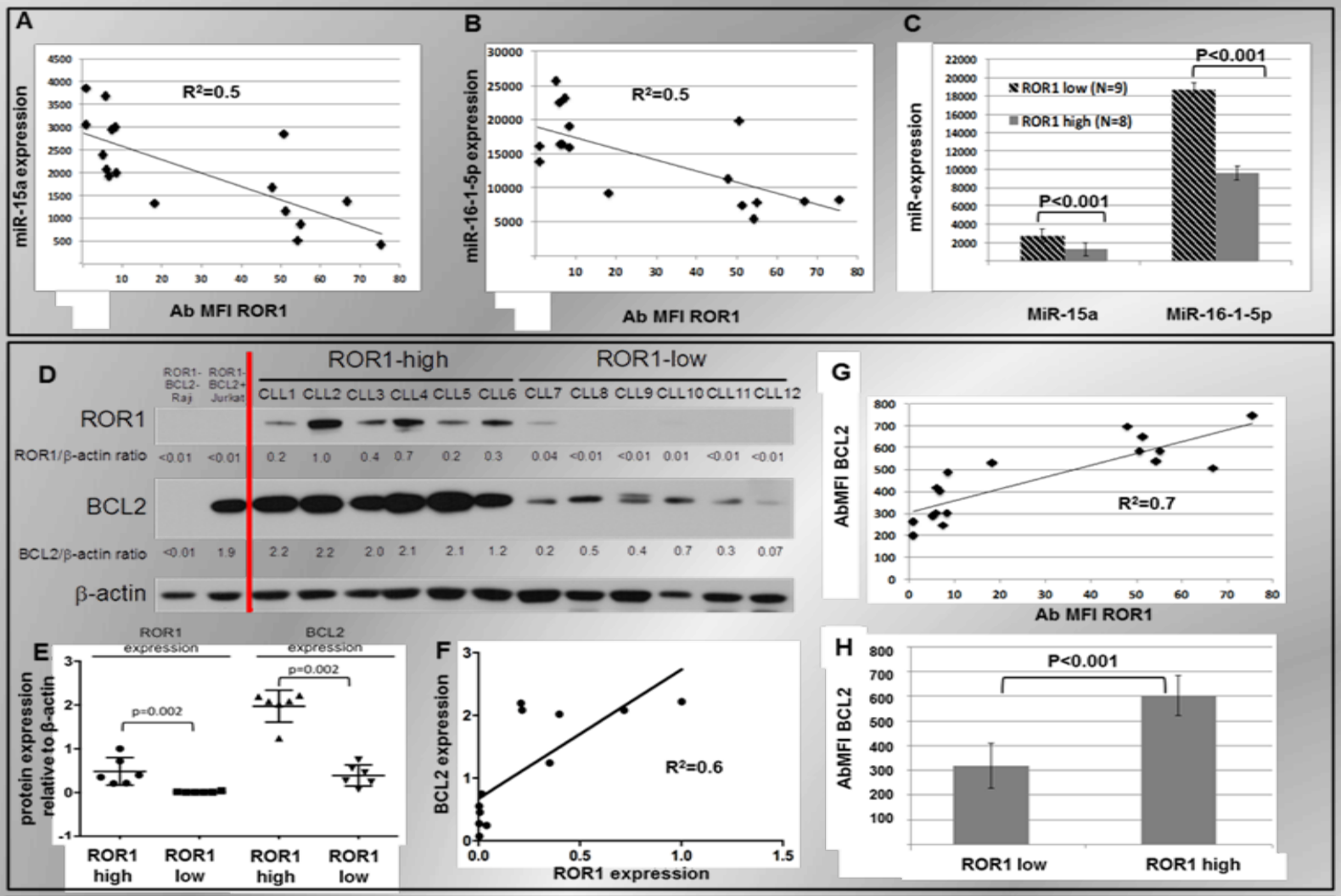

Fig. 4. Expression of miR15/16 ROR1 and BCL2 in CLL. A and B. Reverse correlation of miR15a and miR16-1-5p with ROR1 expression in CLL. C. Graphic representation of data in A and B. D. Correlation between BCL2 and ROR1 expression CLL. Jurkat cell were used as a positive control for BCL2 and Raji cells were used as negative control for BCL2. E. Densitometry analysis of data in D. The Mann Whitney U test was used to calculate p values. F. Correlation between BCL2 and ROR1 expression in CLL samples used in D. G. Correlation between BCL2 and ROR1 expression in CLL samples from the entire cohort A. The Absolute Median Fluorescence Intensity of intracellular BCL2 (AbMFI) is plotted on the Y axis and the AbMFI of surface ROR1 is charted on the X axis. H Graphic representation of data in G.

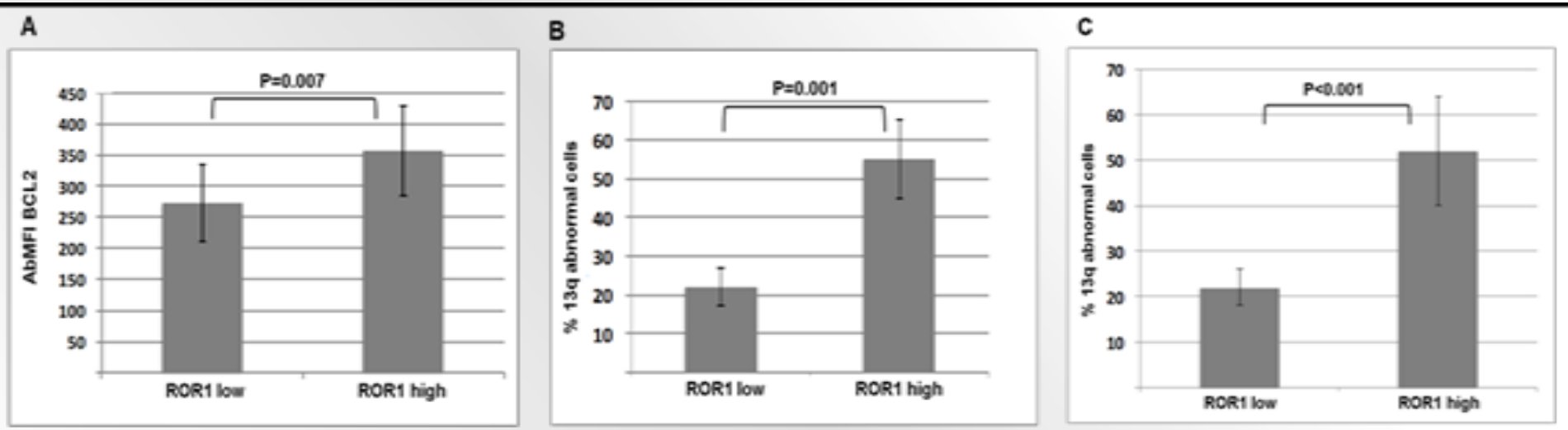

Fig. 5. Relationship between ROR1, BCL2 and percentage of CLL B cells harboring a 13q deletion. Cohort B (N=32) was examined for BCL2 expression and percentage of CLL cells carrying 13q deletion by FISH analysis. A. BCL2 expression in ROR1-low and ROR1-high CLL samples. B. percentage of 13q deleted cells in ROR1-low and ROR1-high CLL samples from cohort B. Samples with low expression of ROR1 had an average expression of intracellular BCL2 of AbMFI=272 (panel A) and the average percentage of CLL B cells carrying a 13q deletion of 22.3 % (panel B). CLL cases with high expression of ROR1 had a mean expression of BCL2 AbMFI=356 (panel A) and had an average % of CLL B cells with a 13q deletion of 55.2% (Panel B). C. percentage of 13q deleted cells in ROR1-low and ROR1-high CLL samples in cohort C, (N=256). CLL samples with low expression of ROR1 had an average of 20.8% of CLL cells carrying 13q deletion. CLL cases with high expression of ROR1 had an average 52% of CLL B cells with 13q deletion.

Cohort A (N=17)	ROR1 low (N=9)	ROR1 high (N=8)
ROR1 (Ave AbMFI)	5.7	53.0
BCL2 (Ave abMFI)	320.3	602.0
Ave % of cells carrying the 13q deletion	5.3	52.1
Median Age at Dx	54.1	60.1
RAI stage at Dx	0 (N=9)	0 (N=6), 1 (N=2)
Ave Time from Dx to sample collection (yrs)	1.8	1.0
Cohort B (N=32)	**ROR1 low (N=19)**	**ROR1 high (N=13)**
ROR1 (Ave AbMFI)	5.1	79.3
BCL2 (Ave abMFI)	272.0	356.4
Ave % of cells carrying the 13q deletion	22.3	55.2
Median Age at Dx	58.0	59.3
RAI stage at Dx	0 (N=12), 1 (N=6), 2 (N=1)	0 (N=9), 1 (N=2), 2 (N=2)
Ave Time from Dx to sample collection (yrs)	1.0	2.1
Cohort C (N=256)	**ROR1 low (N=26)**	**ROR1 high (N=230)**
ROR1 (Ave AbMFI)	5.3	40.1
BCL2 (Ave abMFI)	ND	ND
Ave % of cells carrying the 13q deletion	20.8	52.0
Median Age at Dx	57.5	57.0
RAI stage at Dx	0 (N=19), 1(N=7)	0 (N=160), 1 (N=51), 2 (N=14), 3 (N=2), 4 (N=2)
Ave Time from Dx to sample collection (yrs)	2.7	2.8

Tab. 2. Summary of *ROR1*, *BCL2* (mean AbMFI), and average percentage f cells carrying the 13q deletion. The number of cases with various RAI stages determined at CLL diagnosis, and the average time from diagnosis that the samples were collected and used in this study for the cases in cohorts A, B and C.

Characteristics of 3 CLL samples used for cell viability assay and antibody dependent cellular cytotoxicity assay

Sample ID	Type	ROR1 AbMFI	ZAP-70 (%)	IGHV (%)
CLL1	ROR1 high	56.3	59.0	100
CLL2	ROR1 high	85.0	10.3	100
CLL3	ROR1 high	90.9	2.9	89.3

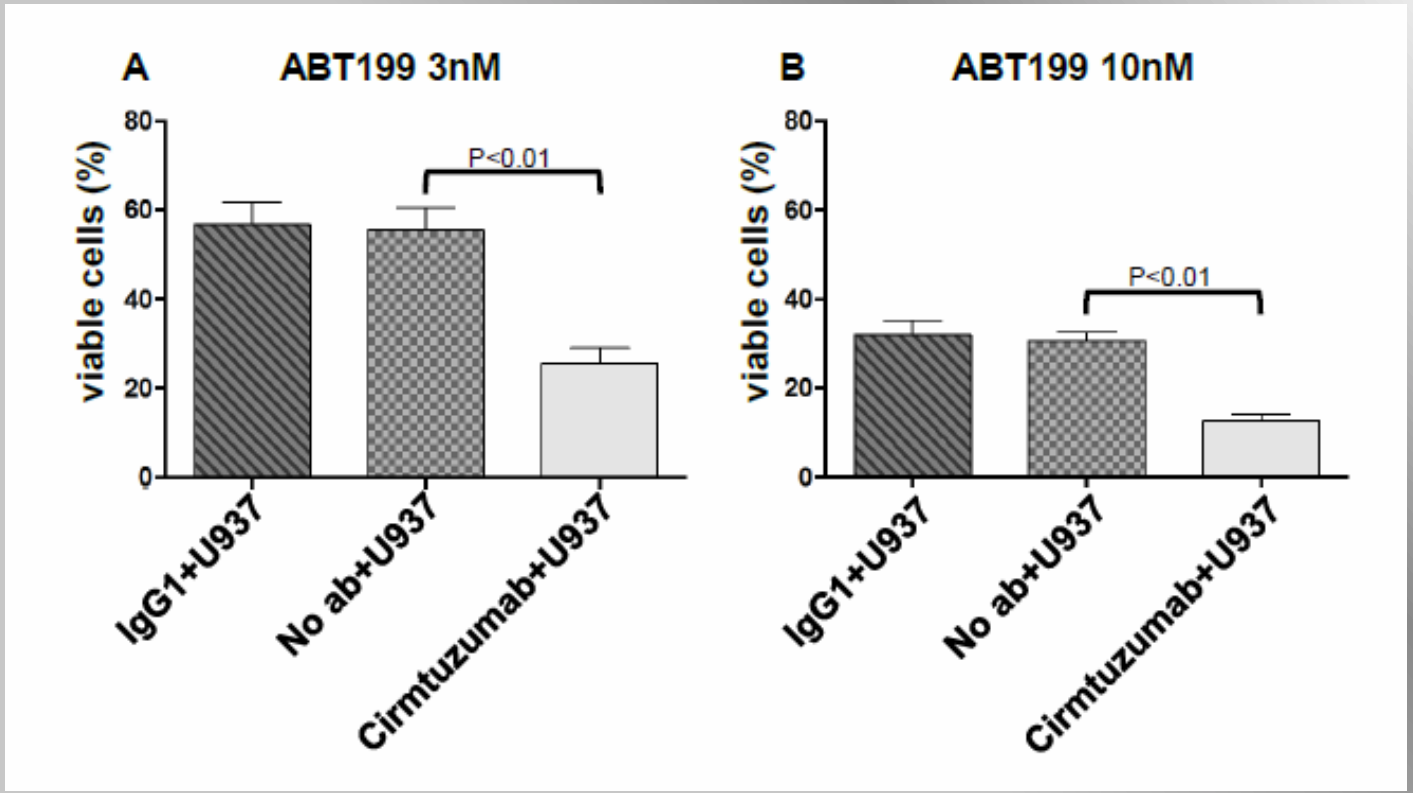

CLL cell viability with U937 effector cells. Bars indicate the average percentage of viable CLL cells normalized with respect to average percentage of viable untreated CLL cells. CLL cell viability is assessed after 16h treatment with 3 nM (**A**) or 10 nM (**B**) Venetoclax either alone or in combination with 20 mg/ml Cirmtuzumab or human IgG1 antibody. U937=human monocyte cell line, No Ab=no antibody control, Cirmtuzumab= anti human *ROR1* antibody, IgG1= anti human IgG1 antibody. Data are shown as mean ± s.e.m.

MicroRNAs targeting 20 bp repeats in *TCL1* 3' UTR

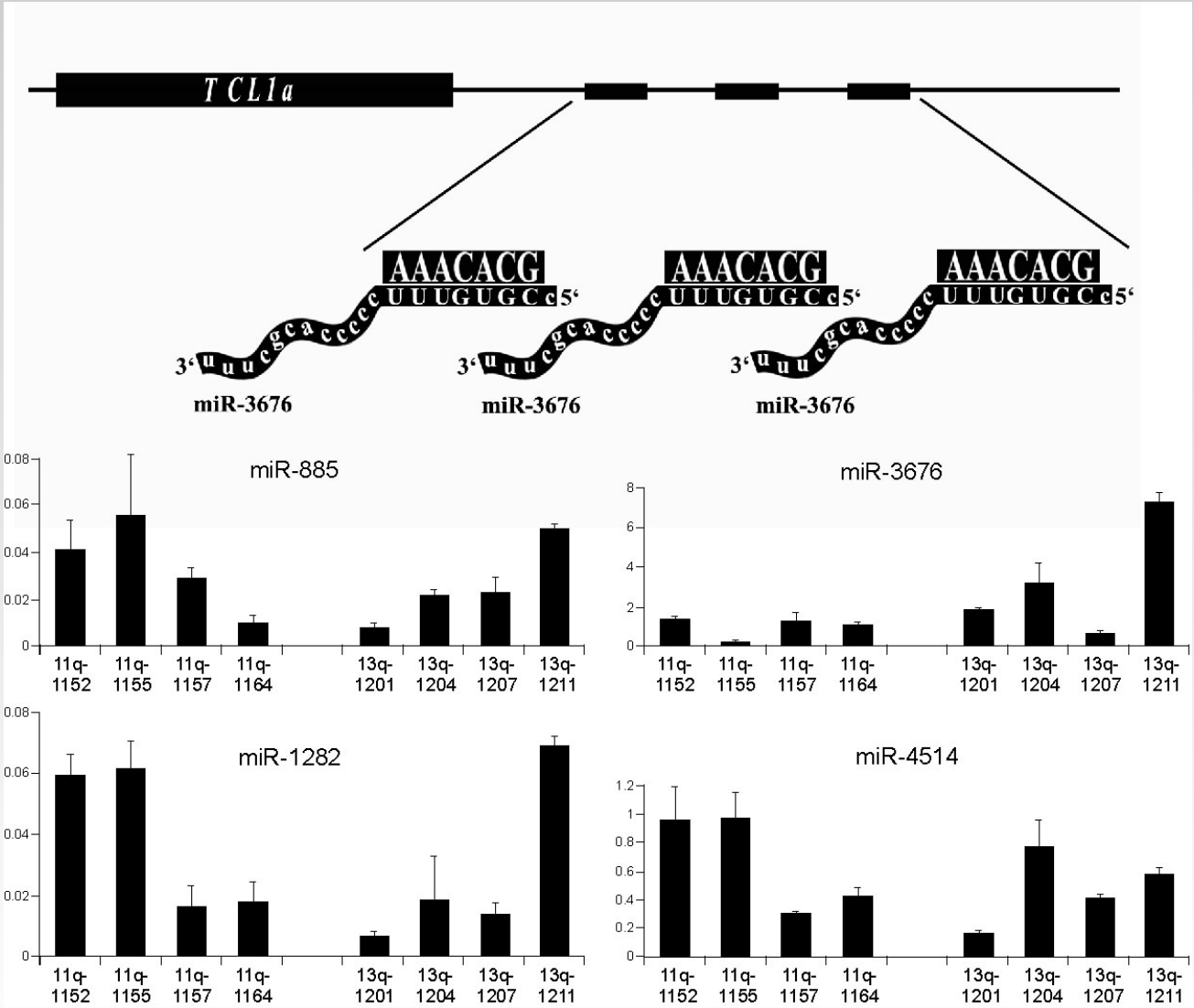

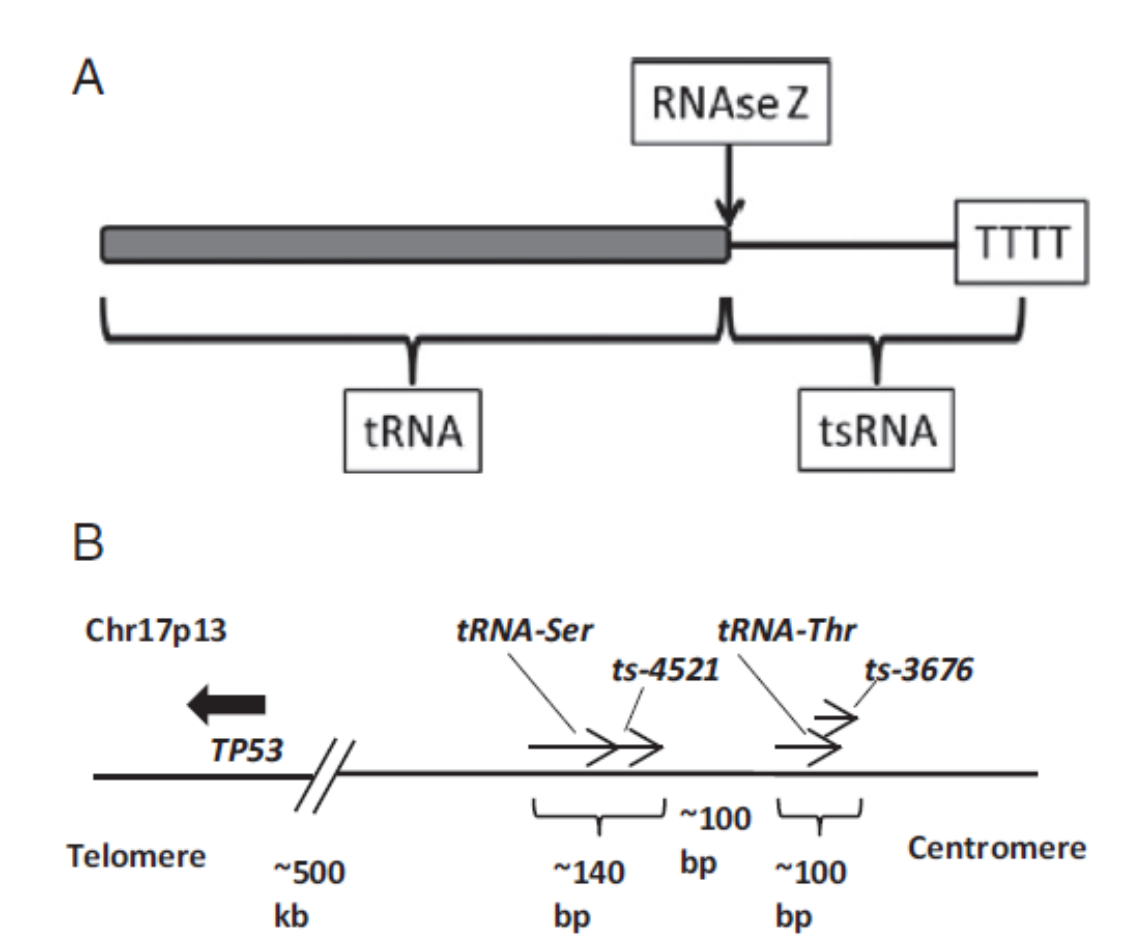

Ts-3676 and *ts-4521* at 17p13.
(A) TsRNAs are produced from the 3′ ends of pre-tRNAs.
(B) Genomic structure of *ts-3676* and *ts-4521.*

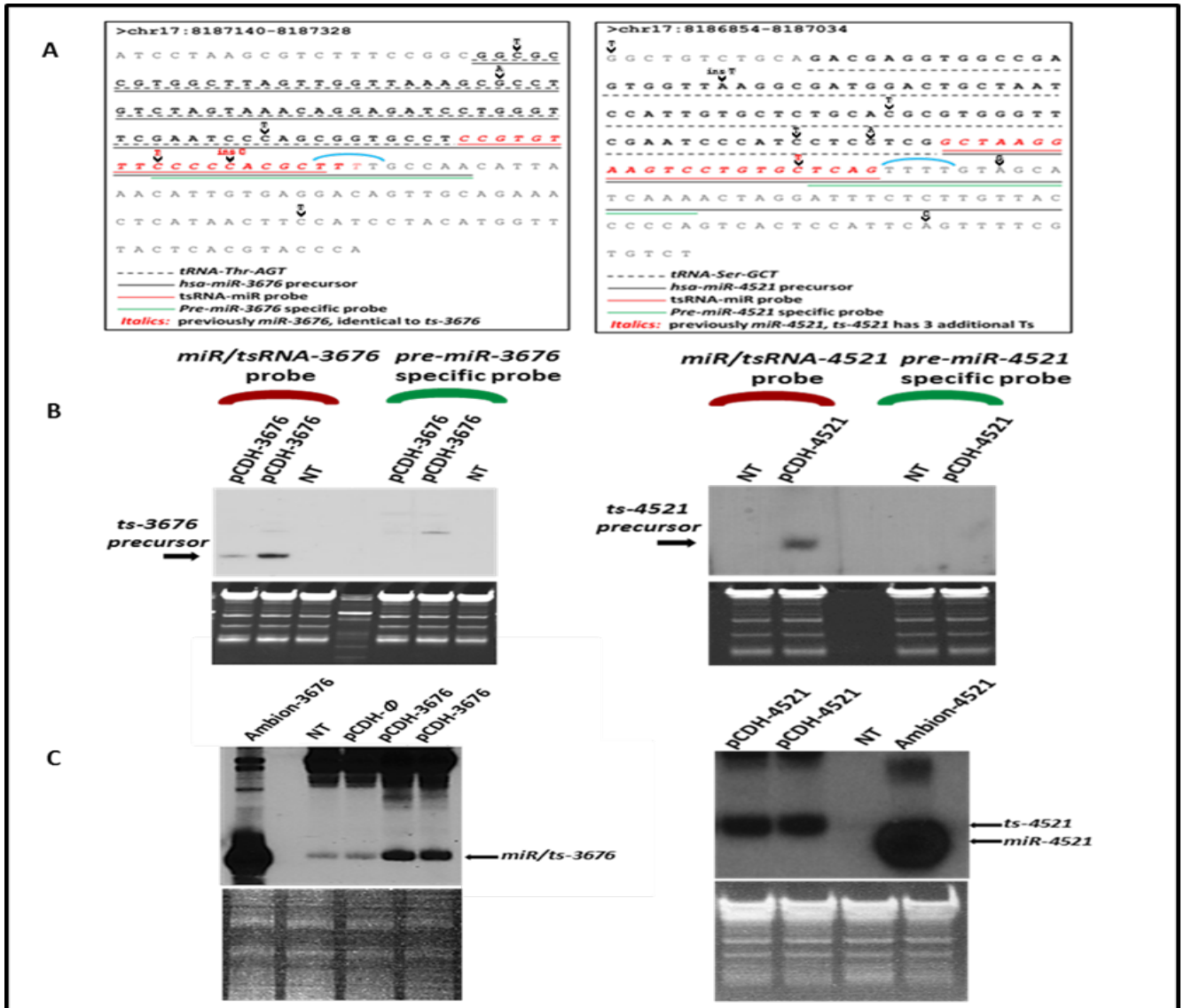

Fig. 6. (A) For both *ts-3676* (left panels) and *ts-4521* (right panels), we designed two probes, one specific for the pre-miR (in green) and one recognizing both miR and tsRNA precursors (in red). The stop codon for RNA polymerase III responsible for tRNA transcription and tsRNA production is marked in blue. We found 5 mutations in *ts-3676* genomic region and 8 mutations in *ts-4521* genomic region (B) The probe specific for the pre-miR (~ 80 bp) does not detect any transcript. The probe designed on the sequence common to both miR and tsRNA shows an ~80 bp signal of a tsRNA precursor indicating that this region produces a tsRNA. (C) TsRNAs produced by the cells transfected with an expression vector and microRNAs produced by the cells transfected with a commercial miR. *Ts-3676* has the same length of the predicted *miR-3676* because the 4 T stretch that represents the RNA pol III stop codon is located exactly at the end of the microRNA sequence. *Ts-4521* have instead a different length, because the 4 T stretch that represents the RNApol III stop codon is located downstream the microRNA sequence.

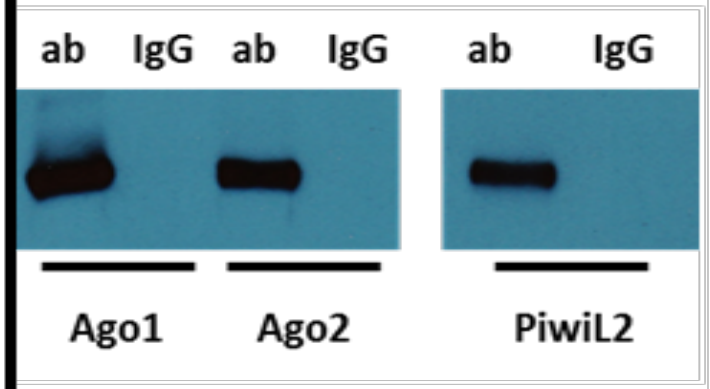

	enrichment (folds) IP-ab vs IP-IgG		
	Ago1	Ago2	PiwiL2
tsRNA/miR-3676	4.95	2.76	2.62
tsRNA-4521	12.34	5.58	2.72
CTRL miR-93	3.16	5.76	N/E
CTRL miR-92	18.79	20.82	N/E

Fig 8. RNA immunoprecipitation experiment using Ago1, Ago2, PiwiL2 (numbers show enrichment folds, N/E indicates no enrichment). Indicated microRNAs/tsRNAs were detected using real time RT-PCR. The western blot performed on the lysates of the RIP obtained with the specific antibody and a control IgG show that the amount of protein immunoprecipitated is equal in each sample.

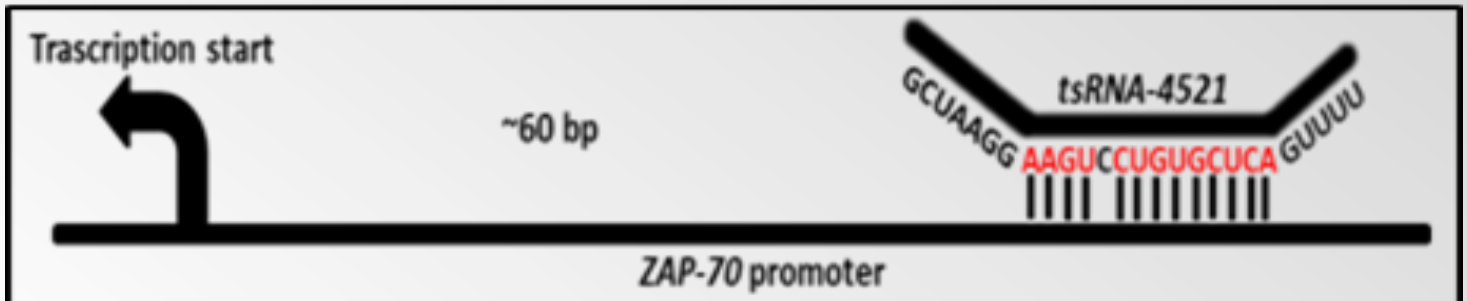

Fig 9. The sequence of *ts-4521* shows a homology of 13 out of 14 bases to the promoter of *ZAP-70* approximatively 60 bases upstream the transcription start site.

A

tsRNA-ID	Linear FC	p-value
ts-3	1.70	0.0001
ts-4	2.02	0.0002
ts-30	1.94	0.0002
ts-26	-1.78	0.0006
ts-43	-3.60	0.0000
ts-46	-4.51	0.0000
ts-47	-4.13	0.0000
ts-49	-1.80	0.0031
ts-53	-1.50	0.0046

B

tsRNA-ID	Linear FC	p-value
ts-4	2.17	0.0000
ts-8	2.00	0.0001
ts-21	2.23	0.0000
ts-30	1.70	0.0009
ts-36	2.88	0.0001
ts-55	2.50	0.0000
ts-53	1.71	0.0001
ts-3	-1.50	0.0006
ts-10	-2.25	0.0000
ts-26	-2.01	0.0000
ts-31	-1.85	0.0000
ts-37	-2.38	0.0004
ts-41	-5.03	0.0000
ts-47	-3.08	0.0000
ts-49	-2.00	0.0003

C

tsRNA-ID	Linear FC	p-value
ts-3	2.55	0.0000
ts-10	1.65	0.0132
ts-31	2.47	0.0000
ts-41	2.85	0.0001
ts-21	-1.63	0.0007
ts-36	-3.11	0.0002
ts-43	-2.56	0.0016
ts-46	-3.52	0.0002
ts-53	-2.55	0.0000
ts-55	-1.93	0.0043

D

tsRNA-ID	Linear FC	P.Value
ts-4	1.41	0.006
ts-10	-2.49	0.005
ts-37	-3.48	0.000
ts-46	-3.32	0.000
ts-47	-5.40	0.000
ts-49	-2.54	0.001

TsRNA signatures in CLL and lung cancer. *(A)* Aggressive CLL vs. normal CD19+ B cells (negative values indicate down-regulation in CLL). *(B)* Aggressive CLL vs. indolent CLL (negative values indicate down-regulation in aggressive CLL). *(C)* Indolent CLL vs. normal CD19+ B cells (negative values indicate downregulation in CLL). (D) Lung cancer cells vs. normal lung (negative values indicate down-regulation in lung cancer).